Deep learning-based semantic segmentation of tomato leaf diseases using U-Net and classification of blight using ResNet

Asha Mangala Shankaregowda[1,2,3], Yogish Hullukere Kadegowda[2,3]
[1]Department of Computer Science and Engineering, CHRIST University, Bengaluru, India
[2]Department of Information Science and Engineering, Ramaiah Institute of Technology, Bengaluru, India
[3]Department of Information Science and Engineering, Ramaiah Institute of Technology, Visvesvaraya Technological University, Belagavi, India

Article Info

Article history:

Received Sep 23, 2024
Revised Jan 30, 2025
Accepted Mar 3, 2025

Keywords:

Deep learning
Plant disease detection
ResNet18
Tomato leaf diseases
U-Net

ABSTRACT

Effective disease control requires the early identification and diagnosis of plant diseases, especially those affecting tomato leaves. A crucial stage in this process is segmenting images of diseased leaves, but this can be difficult because of the uneven shapes, varied sizes, vibrant colors, and frequently blurry borders of the affected portions, in addition to the messy backgrounds. We propose a deep learning-based strategy based on the U-Net architecture for addressing these issues, enabling precise segmentation and timely identification of tomato leaf diseases. With a DICE score of 0.93 and an accuracy of 93% in identifying healthy from diseased locations, this technique shows promise in helping farmers carry out focused interventions. Furthermore, the ResNet18 model has good levels of specificity, sensitivity, and accuracy when used to classify early and late blight. These outcomes highlight the way our suggested models perform in actual agricultural environments. Subsequent research endeavors will center on augmenting the model's generalizability in various agricultural settings and investigating multi-modal imaging methodologies. It is also intended for the advancement of mobile applications and edge computing to enable real-time disease monitoring and sustainable farming methods worldwide.

Corresponding Author:

Asha Mangala Shankaregowda
Department of Computer Science and Engineering, CHRIST University
Bengaluru, Karnataka, India
Email: ashagowda05@gmail.com

1. INTRODUCTION

One of the most important crops in the world in terms of economic impact is the tomato (*Solanum Lycopersicon*), which adds vital nutrients and tastes to a wide range of diets. Tomato plants are prone to a number of illnesses, though, and this can negatively affect growers' profits, productivity, and quality. Tomato mosaic virus, powdery mildew, early and late blight, bacterial spot, and tomato blight are among the common diseases that harm tomato leaves [1]–[3]. The signs of these diseases include lesions, spots, discoloration, wilting, and deformities on the leaves. Eventually, these conditions result in a decrease in photosynthetic capability and hampered fruit development [4]–[7]. Early detection and management of these diseases are paramount for maintaining the health and productivity of tomato crops. Timely intervention strategies, such as targeted pesticide application, crop rotation, and resistant cultivar selection, can mitigate the spread and severity of diseases, thereby minimizing yield losses and ensuring food security.

In recent years, advancements in artificial intelligence, particularly deep learning, have revolutionized various fields, including computer vision and agriculture. Deep learning techniques, especially convolutional neural networks (CNNs), have shown remarkable performance in image recognition, object detection, and semantic segmentation tasks. Semantic segmentation, a pixel-level classification method, assigns each pixel in an image to a specific class label, enabling detailed understanding and analysis of visual data [8]–[16].

Among CNN-based architectures, U-Net has emerged as a powerful tool for semantic segmentation tasks, particularly in biomedical imaging and agricultural applications. The U-Net architecture comprises an encoder-decoder framework with symmetric contracting and expansive pathways, featuring skip connections that bridge corresponding layers of the encoder and decoder. This design facilitates the propagation of high-resolution feature maps from the encoder to the decoder, enabling precise localization and segmentation of objects in images [17], [18].

Deep residual learning is used by ResNet18, a residual network (ResNet) architectural variation, to help in the training of extremely deep neural networks. It uses residual blocks and has eighteen layers, including convolutional, pooling, and fully connected layers. A shortcut link that skips one or more levels and a set of convolutional layers are present in every residual block. By permitting gradients to pass straight through the network, this shortcut, also known as a skip link, solves the vanishing gradient issue and preserves signal strength while enhancing training effectiveness. The architecture’s ability to maintain performance in deep networks without degradation is primarily attributed to these residual connections, enabling ResNet18 to achieve high accuracy on complex image recognition tasks while remaining computationally efficient [19]–[25].

Our approach achieves great precision and accuracy by accurately segmenting fatigued regions in tomato leaf images using a U-Net architecture. It ensures high specificity and sensitivity by classifying early and late blight using the ResNet18 model. This method improves sustainable farming practices by helping farmers treat diseases in a timely and focused manner.

2. METHOD

2.1. Dataset

The dataset used, comprises images of tomato leaves exhibiting various disease symptoms. A total of 2809 images were collected, capturing a diverse range of disease manifestations, including lesions, spots, discoloration, and deformities. These images were obtained from a Kaggle challenge. Each image in the dataset is accompanied by a corresponding ground truth mask delineating the unhealthy regions on the tomato leaves. These masks were manually annotated. The annotation process involved meticulous inspection and labeling of disease symptoms, ensuring comprehensive coverage of all affected regions.

For training the segmentation model, 2,809 images from the dataset were utilized, with their respective ground truth masks serving as the target labels for supervised learning. The training dataset includes a balanced distribution of images containing different disease types and severity levels, accounting for robust model training and generalization. To evaluate the performance of the segmentation model, a separate test set consisting of 100 images was curated. These test images were selected to encompass a wide range of disease scenarios encountered in practical agricultural settings, including common diseases such as bacterial spot, early blight and late blight. The corresponding ground truth masks for the test set were also provided to assess the model's accuracy and generalization capabilities on unseen data.

The dataset undergoes preprocessing steps to ensure consistency and compatibility with the segmentation model. This includes resizing all images to a uniform resolution of 256×256 pixels, normalization to standardize pixel intensity values, and augmentation techniques such as random rotations, flips, and scaling to enhance the diversity of training samples and improve model robustness. The dataset utilized for classification of blight in this study is categorized into two distinct classes, early blight and late blight, consisting of 929 images of early blight and 1,780 images of late blight. To facilitate robust evaluation, a test set was meticulously curated, comprising 100 images, with an equal representation of 50 images from each class. Also in this study evaluation, a carefully selected test set data for both potato and maize leaves were also used.

2.2. Network architecture

The deep learning architecture used in this study is the standard U-Net, a convolutional neural network specifically designed for semantic segmentation tasks. U-Net architecture captures contextual information while preserving spatial details. The U-Net architecture comprises an encoder-decoder framework with skip connections, as shown in Figure 1.

The encoder route is made up of a series of convolutional and pooling layers that minimize spatial dimensions while capturing hierarchical characteristics. Repaired linear unit (ReLU) activation functions trail each convolutional layer, enabling non-linear transformations. The decoder route, which consists of up-convolutional layers to gradually regain spatial resolution, symmetrically mirrors the encoder. By creating skip links between the encoder and decoder's appropriate layers, feature maps may flow directly across different resolution levels. These skip connections are essential for enabling accurate object localization and segmentation by fusing the encoder's high-resolution feature maps with the decoder's low-resolution feature maps. In the context of U-Net architecture, "copy and crop" refers to the process of copying, cropping, and concatenating feature maps from the contracting (down sampling) path with feature maps from the expanding (up sampling) path. By preserving spatial information and combining high-level data from later layers with low-level characteristics from earlier layers, this improves segmentation accuracy.

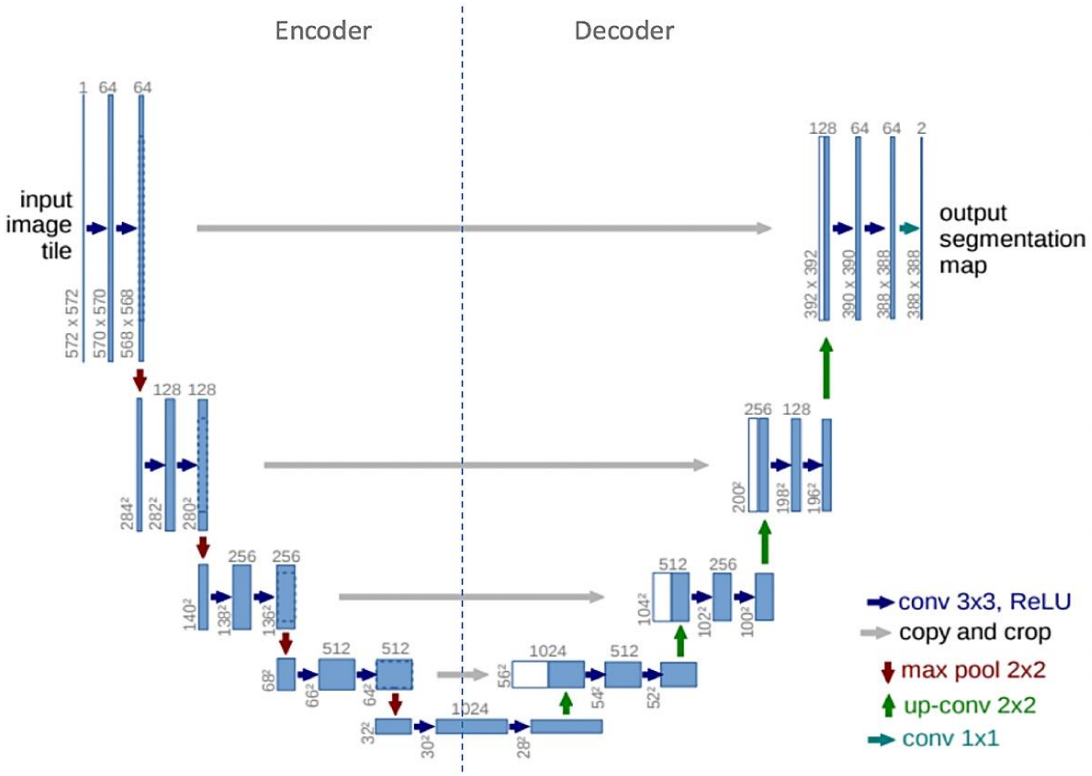

Figure1. U-Net architecture

To fine-tune and localize the segmented objects, the concatenated feature maps go through further convolutional processes and activation functions at each decoding phase. While dropout layers may be inserted to reduce overfitting and enhance model generalization, batch normalization layers are included throughout the network to stabilize and speed up the training process.

The last layer in the U-Net architecture creates pixel-wise probability maps by using a sigmoid activation function to show how likely it is that each pixel is part of the target class (*e.g.*, healthy or sick patches on tomato leaves). Through training, the model compares the predicted probability maps with the ground truth masks in order to learn how to minimize a predetermined loss function, such as DICE loss was calculated using (1) and (2) as depicted below.

$$L = -\frac{1}{n}\sum_{i=1}^{n}(y_i \log(z_i) + (1 - y_i)\log(1 - z_i)) \quad (1)$$

Where n is the number of pixels, y_i is the ground truth label for pixel I (0 or 1 for binary segmentation), z_i is the predicted probability for pixel i.

$$L = 1 - \frac{\sum_{i=1}^{n} y_i z_i}{\sum_{i=1}^{n} y_i + \sum_{i=1}^{n} z_i} \quad (2)$$

Where y_i is the ground truth for pixel i, z_i is the predicted value for pixel i.

Figure 2 representation of the ResNet18 architecture shows its 18 layers-convolutional, pooling, and fully linked layers-arranged into a sequence of residual blocks. In ResNet18, each residual block is composed of two convolutional layers, batch normalization, and a ReLU activation function. The identity shortcut connections that allow the input to bypass one or more levels and be added directly to the output are what make these blocks special. Because the gradients may travel through the identity connections directly during backpropagation, this bypassing method substantially mitigates the vanishing gradient problem. This preserves the signal intensity and makes it easier to train even deeper networks.

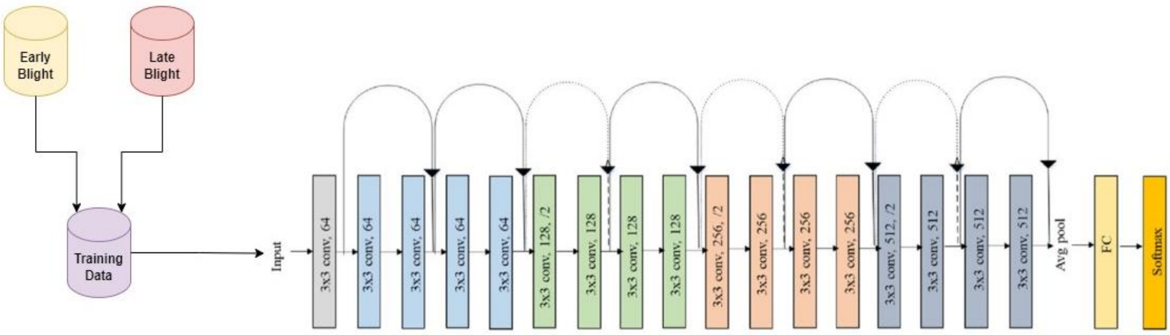

Figure 2. ResNet18 architecture for classifying blight

The architecture is structured as follows: the initial layer is a 7×7 convolutional layer with 64 filters and a stride of 2, followed by a 3×3 max-pooling layer with a stride of 2. Subsequently, there are four stages, each containing two residual blocks. The first stage includes two blocks with 64 filters, the second stage has two blocks with 128 filters, the third stage contains two blocks with 256 filters, and the fourth stage consists of two blocks with 512 filters. To decrease the spatial dimensions of the feature maps, the initial convolution in the residual block has a stride of 2 in phases where the number of filters rises. A fully linked layer with SoftMax activation for classification and a global average pooling layer complete the network. The SoftMax activation function is used for the classification tasks in this study in order to differentiate between early and late blight in tomato leaves. SoftMax is used to transform the output logits into probability distributions so that the model can forecast the class with the highest probability.

This residual learning framework allows ResNet18 to maintain high performance even with increased depth, as the residual connections provide a direct path for the gradient flow, thus enhancing the convergence rate and accuracy of the model. These architectural advances are utilized in this study's application of ResNet18 to provide effective and precise picture classification, with a specific focus on differentiating between early and late blight in plant photos. The network is a good fit for this challenging classification task because of its resilience and feature extraction effectiveness.

2.3. Training methods

The U-Net model was trained for 100 epochs. During training, the DICE loss function was employed as the loss function. The DICE loss quantifies the similarity between predicted and ground truth segmentation masks, guiding the model towards precise segmentation of diseased areas on tomato leaves. To optimize the model parameters, the Adam optimizer was used.

50 epochs were used to train the ResNet model. The loss function that was employed was binary cross entropy loss. Starting in the 40th epoch, early stopping was instituted. The 35th period produced the best model. Although this optimized model was initially trained on tomato leaves, its effectiveness was subsequently assessed on the potato and maize leaf datasets.

3. RESULTS

Figure 3 shows the evolution of the loss curve over 100 training epochs, illustrating the U-Net segmentation model's training process for tomato leaf disease detection. The loss function steadily decreases as the loss curve displays the distinctive “L” shape, which is consistent with the general trend seen during deep learning model training as shown in Figure 3. The DICE score and accuracy are the assessment metrics that are used to evaluate the segmentation model's performance. These measurements shed insight into how well the algorithm distinguishes sick areas on tomato leaves.

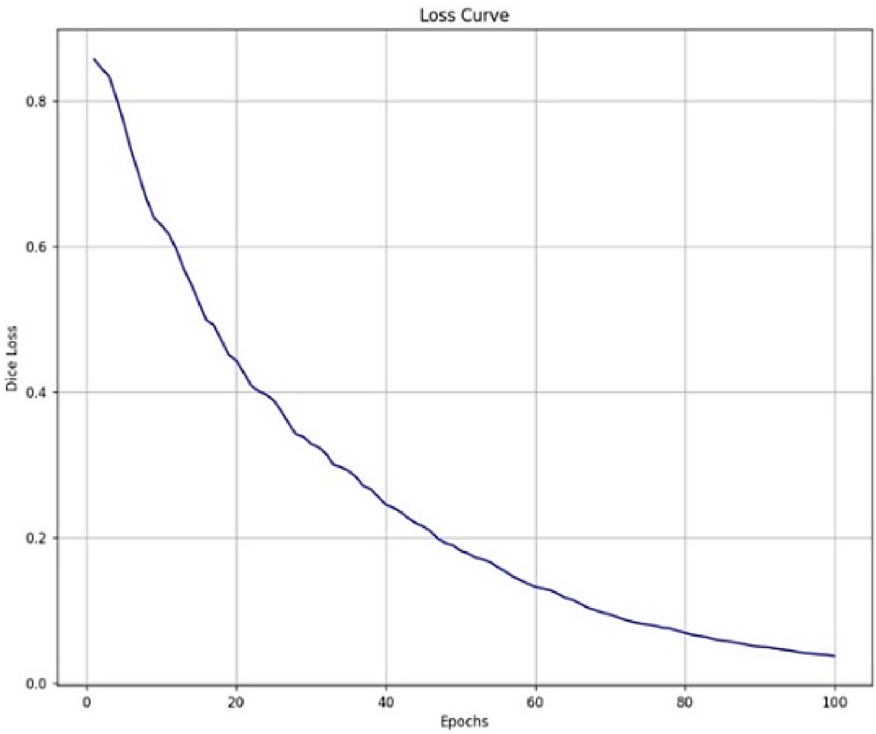

Figure 3. Loss curve

Table 1 summarizes the segmentation model's accuracy, which was 92.5%, and its DICE score, which was 0.93. While the DICE score measures the overlap between the anticipated and ground truth masks, offering a reliable indicator of segmentation accuracy, the accuracy metric shows the proportion of properly identified pixels in the segmentation masks.

Table 1. Performance metrics for Tomato dataset

Metric	Value
Accuracy	92.5%
DICE score	0.93

A test set of 100 images, equally represented by 50 images from each class, was used to assess the ResNet18 model's effectiveness in differentiating between early and late blight. The sensitivity, specificity, and accuracy of the model's predictions were assessed, and for each of the three datasets, a confusion matrix and receiver operating characteristic (ROC) curve were used to visualize the results. The confusion matrix, depicted in Figure 4, summarizes the classification outcomes. The model correctly identified 47 out of 50 early blight cases and 48 out of 50 late blight cases from Tomato leaf dataset. The confusion matrix, depicted in Figure 5(a), summarizes the classification outcomes. The model correctly identified 44 out of 50 early blight cases and 45 out of 50 late blight cases from Potato leaf dataset. The confusion matrix, depicted in Figure 5(b), summarizes the classification outcomes. The model correctly identified 41 out of 50 early blight cases and 42 out of 50 late blight cases from Maize leaf dataset.

The sensitivity and specificity, or true positive and true negative rates, were computed from the confusion matrix. 96% of real late blight instances were found to be successfully detected, which is known as the sensitivity. 94% of true early blight cases were successfully recognized, according to the specificity. Using the Tomato Leaf dataset, the model's overall accuracy-which is measured as the percentage of properly identified occurrences among all instances-was 95%. The accuracy, specificity, and sensitivity for three distinct datasets are shown in Figure 6.

The ROC curve for Tomato leaf dataset, shown in Figure 7, illustrates the model's diagnostic ability. AUC was calculated to be 0.95, indicating a high level of discriminative power between the two classes. The ROC curve demonstrates that the model performs consistently well across various threshold levels.

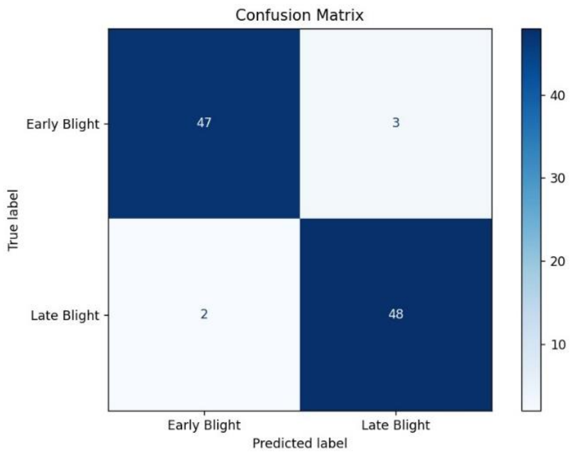

Figure 4. Confusion matrix for early blight and late blight Tomato dataset

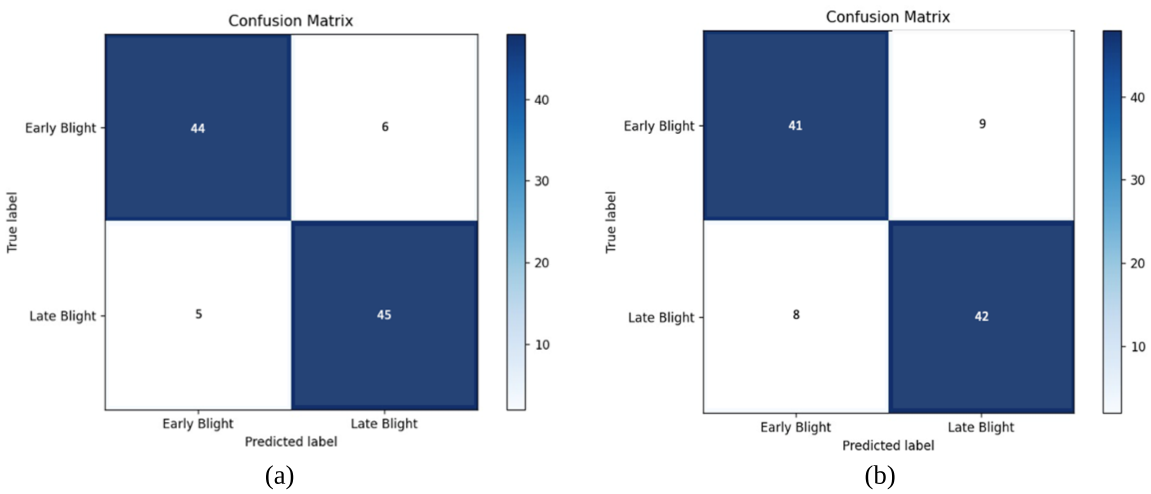

Figure 5. Confusion matrix for early blight and late blight for (a) Potato dataset and (b) Maize dataset

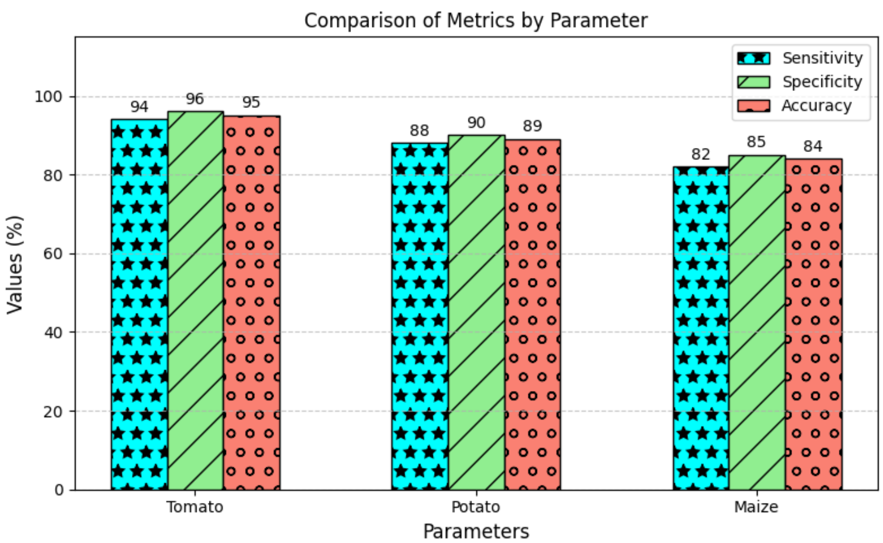

Figure 6. Sensitivity, specificity and accuracy plots for various leaf datasets

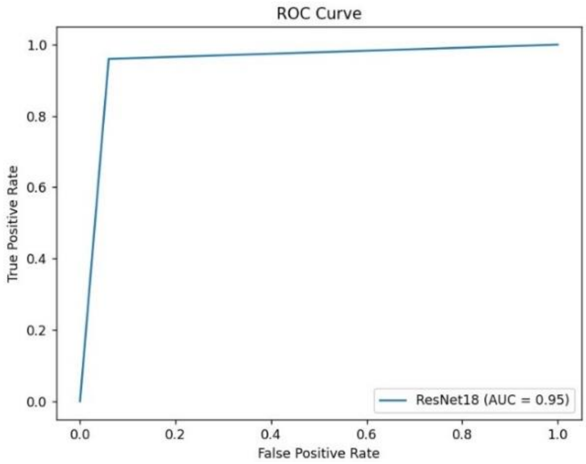

Figure 7. AUC and ROC curve

4. DISCUSSION

The utilization of the U-Net architecture in this study has showed promising outcomes for early detection and precise mapping of tomato leaf diseases. With an accuracy of 92.5% and a DICE score of 0.93, the model effectively distinguished between healthy and diseased regions, demonstrating its potential to aid farmers in implementing targeted intervention strategies. This application of deep learning-based segmentation techniques holds significant implications for sustainable agriculture, empowering farmers with timely information to optimize resource utilization and mitigate yield losses.

The assessment findings show that the ResNet18 model performs well across three datasets: tomato, potato, and maize leaves, for both the early blight and late blight classification tasks. With respect to the tomato leaf dataset, the model achieved a 95% accuracy rate by accurately identifying 47 out of 50 early blight photos and 48 out of 50 late blight images. This high accuracy rate shows that the model can generalize effectively to new, unobserved data, which makes it a useful tool for real-world plant disease detection applications. The model's ability to accurately identify cases of late blight, which is essential to stopping the spread of this more aggressive blight type, is demonstrated by its sensitivity of 0.96. Similarly, the specificity of 0.94 demonstrates the model's effectiveness in accurately detecting early blight, thereby reducing false positives and ensuring that healthy plants are not mistakenly treated for late blight. The ROC curve and the corresponding AUC of 0.95 further corroborate the model's excellent discriminative capabilities. The ROC curve illustrates that the ResNet18 model maintains a high true positive rate while keeping the false positive rate low across different threshold settings, which is essential for making reliable predictions in varying operational scenarios.

Similar results were obtained for the potato leaf dataset, where the model achieved an accuracy of 89% by accurately identifying 44 out of 50 early blight photos and 45 out of 50 late blight images. The ROC AUC of 0.89 for this dataset also shows the sensitivity and specificity, suggesting strong performance in differentiating between early and late blight. Because of its great accuracy, the model may also be trusted to identify potato leaf blight, hence assisting disease control initiatives. For the maize leaf dataset, the model correctly identified 41 out of 50 early blight images and 42 out of 50 late blight images, achieving an accuracy of 83%. The ROC AUC of 0.83, while slightly lower than the other datasets, still signifies a solid performance in differentiating between the types of blight. The model’s consistent performance across different crops showcases its versatility and robustness in plant disease detection, making it a valuable asset for agricultural disease management.

These results underscore the model's overall reliability and effectiveness, demonstrating its potential for broad application in agricultural disease detection and management. Moving forward, future research endeavors could explore avenues to enhance model generalization across diverse agricultural contexts and integrate multi-modal imaging techniques for comprehensive disease diagnosis. The adoption of these technologies could be further accelerated by efforts to develop mobile and edge computing solutions for in-the-field real-time disease monitoring (such as drone-based monitoring systems), which would ultimately strengthen and sustain agricultural systems across the globe.

5. CONCLUSION

This work demonstrates the effectiveness of deep learning models in early detection and categorization of tomato, potato, and maize leaf diseases. Precise identification of afflicted locations was made possible by the U-Net architecture's excellent accuracy and DICE scores. Impressive sensitivity, specificity, and overall accuracy were demonstrated by the ResNet18 model in its classification of early and late blight across all three datasets. For tomato leaves, the model achieved 95% accuracy, with a sensitivity of 0.96 and specificity of 0.94. For potato leaves, the model resulted in 89% accuracy and an ROC AUC of 0.89. About maize leaves, the model's accuracy was 83%, and its ROC AUC was 0.83. These findings demonstrate how these models, which offer accurate and dependable disease detection and classification for many crops, might enhance agricultural disease control strategies. Future research should concentrate on enhancing model generalization across various crops and using cutting-edge imaging techniques to further maximize real-time, in-field disease monitoring and intervention.

FUNDING INFORMATION

Authors state no funding involved.

AUTHOR CONTRIBUTIONS STATEMENT

This journal uses the Contributor Roles Taxonomy (CRediT) to recognize individual author contributions, reduce authorship disputes, and facilitate collaboration.

Name of Author	C	M	So	Va	Fo	I	R	D	O	E	Vi	Su	P	Fu
Asha Mangala Shankaregowda		✓		✓				✓	✓	✓				
Yogish Hullukere Kadegowda					✓					✓		✓		

C : **C**onceptualization
M : **M**ethodology
So : **So**ftware
Va : **Va**lidation
Fo : **Fo**rmal analysis
I : **I**nvestigation
R : **R**esources
D : **D**ata Curation
O : Writing - **O**riginal Draft
E : Writing - Review & **E**diting
Vi : **Vi**sualization
Su : **Su**pervision
P : **P**roject administration
Fu : **Fu**nding acquisition

CONFLICT OF INTEREST STATEMENT

Authors state no conflict of interest.

INFORMED CONSENT

The authors confirm that all data used in this study, including images of tomato leaves, were publicly available. No human participants or personal data were involved in this study.

ETHICAL APPROVAL

The authors affirm that the research was conducted in accordance with ethical standards and institutional guidelines.

DATA AVAILABILITY

The data that support the findings of this study are openly available in Kaggle at *https://www.kaggle.com/datasets/charuchaudhry/plantvillage-tomato-leaf-dataset*.

REFERENCES

[1] M. Sigala, A. Beer, L. Hodgson, and A. O'Connor, *Big data for measuring the impact of tourism economic development programmes: A process and quality criteria framework for using big data*. 2019. doi: 10.1007/978-981-13-6339-9_4.

[2] G. Nguyen *et al.*, "Machine learning and deep learning frameworks and libraries for large-scale data mining: A survey," *Artificial Intelligence Review*, vol. 52, no. 1, pp. 77–124, 2019, doi: 10.1007/s10462-018-09679-z.

[3] C. Shorten and T. M. Khoshgoftaar, "A survey on image data augmentation for deep learning," *Journal of Big Data*, vol. 6, no. 1, 2019, doi: 10.1186/s40537-019-0197-0.

[4] R. Vinayakumar, M. Alazab, K. P. Soman, P. Poornachandran, A. Al-Nemrat, and S. Venkatraman, "Deep learning approach for intelligent intrusion detection system," *IEEE Access*, vol. 7, pp. 41525–41550, 2019, doi: 10.1109/ACCESS.2019.2895334.

[5] K. Sivaraman, R. M. V. Krishnan, B. Sundarraj, and S. Sri Gowthem, "Network failure detection and diagnosis by analyzing

syslog and SNS data: Applying big data analysis to network operations," *International Journal of Innovative Technology and Exploring Engineering*, vol. 8, no. 9 Special Issue 3, pp. 883–887, Aug. 2019, doi: 10.35940/ijitee.I3187.0789S319.
[6] A. D. Dwivedi, G. Srivastava, S. Dhar, and R. Singh, "A decentralized privacy-preserving healthcare blockchain for IoT," *Sensors (Switzerland)*, vol. 19, no. 2, pp. 1–17, 2019, doi: 10.3390/s19020326.
[7] F. Al-Turjman, H. Zahmatkesh, and L. Mostarda, "Quantifying uncertainty in internet of medical things and big-data services using intelligence and deep learning," *IEEE Access*, vol. 7, pp. 115749–115759, 2019, doi: 10.1109/ACCESS.2019.2931637.
[8] L. M. Ang, K. P. Seng, G. K. Ijemaru, and A. M. Zungeru, "Deployment of IoV for smart cities: Applications, architecture, and challenges," *IEEE Access*, vol. 7, pp. 6473–6492, 2019, doi: 10.1109/ACCESS.2018.2887076.
[9] S. Kumar and M. Singh, "Big data analytics for healthcare industry: Impact, applications, and tools," *Big Data Mining and Analytics*, vol. 2, no. 1, pp. 48–57, 2019, doi: 10.26599/BDMA.2018.9020031.
[10] B. P. L. Lau *et al.*, "A survey of data fusion in smart city applications," *Information Fusion*, vol. 52, no. January, pp. 357–374, 2019, doi: 10.1016/j.inffus.2019.05.004.
[11] Y. Wu *et al.*, "Large scale incremental learning," *Proceedings of the IEEE Computer Society Conference on Computer Vision and Pattern Recognition*, vol. 2019-June, pp. 374–382, 2019, doi: 10.1109/CVPR.2019.00046.
[12] A. Mosavi, S. Shamshirband, E. Salwana, K. wing Chau, and J. H. M. Tah, "Prediction of multi-inputs bubble column reactor using a novel hybrid model of computational fluid dynamics and machine learning," *Engineering Applications of Computational Fluid Mechanics*, vol. 13, no. 1, pp. 482–492, 2019, doi: 10.1080/19942060.2019.1613448.
[13] V. Palanisamy and R. Thirunavukarasu, "Implications of big data analytics in developing healthcare frameworks – A review," *Journal of King Saud University - Computer and Information Sciences*, vol. 31, no. 4, pp. 415–425, 2019, doi: 10.1016/j.jksuci.2017.12.007.
[14] J. Sadowski, "When data is capital: datafication, accumulation, and extraction," *Big Data and Society*, vol. 6, no. 1, pp. 1–12, 2019, doi: 10.1177/2053951718820549.
[15] J. R. Saura, B. R. Herraez, and A. Reyes-Menendez, "Comparing a traditional approach for financial brand communication analysis with a big data analytics technique," *IEEE Access*, vol. 7, pp. 37100–37108, 2019, doi: 10.1109/ACCESS.2019.2905301.
[16] D. Nallaperuma *et al.*, "Online incremental machine learning platform for big data-driven smart traffic management," *IEEE Transactions on Intelligent Transportation Systems*, vol. 20, no. 12, pp. 4679–4690, 2019, doi: 10.1109/TITS.2019.2924883.
[17] S. Schulz, M. Becker, M. R. Groseclose, S. Schadt, and C. Hopf, "Advanced MALDI mass spectrometry imaging in pharmaceutical research and drug development," *Current Opinion in Biotechnology*, vol. 55, pp. 51–59, 2019, doi: 10.1016/j.copbio.2018.08.003.
[18] C. Shang and F. You, "Data analytics and machine learning for smart process manufacturing: Recent advances and perspectives in the big data era," *Engineering*, vol. 5, no. 6, pp. 1010–1016, 2019, doi: 10.1016/j.eng.2019.01.019.
[19] Y. Yu, M. Li, L. Liu, Y. Li, and J. Wang, "Clinical big data and deep learning: Applications, challenges, and future outlooks," *Big Data Mining and Analytics*, vol. 2, no. 4, pp. 288–305, 2019, doi: 10.26599/BDMA.2019.9020007.
[20] M. Huang, W. Liu, T. Wang, H. Song, X. Li, and A. Liu, "A queuing delay utilization scheme for on-path service aggregation in services-oriented computing networks," *IEEE Access*, vol. 7, pp. 23816–23833, 2019, doi: 10.1109/ACCESS.2019.2899402.
[21] G. Xu, Y. Shi, X. Sun, and W. Shen, "Internet of things in marine environment monitoring: A review," *Sensors (Switzerland)*, vol. 19, no. 7, pp. 1–21, 2019, doi: 10.3390/s19071711.
[22] M. Aqib, R. Mehmood, A. Alzahrani, I. Katib, A. Albeshri, and S. M. Altowaijri, *Smarter traffic prediction using big data, in-memory computing, deep learning and gpus*, vol. 19, no. 9. 2019. doi: 10.3390/s19092206.
[23] S. Leonelli and N. Tempini, *Data journeys in the sciences*. 2020. doi: 10.1007/978-3-030-37177-7.
[24] N. Stylos and J. Zwiegelaar, *Big data as a game changer: How does it shape business intelligence within a tourism and hospitality industry context?* 2019. doi: 10.1007/978-981-13-6339-9_11.
[25] Q. Song, H. Ge, J. Caverlee, and X. Hu, "Tensor completion algorithms in big data analytics," *ACM Transactions on Knowledge Discovery from Data*, vol. 13, no. 1, pp. 1–48, Jan. 2019, doi: 10.1145/3278607.

BIOGRAPHIES OF AUTHORS

Asha Mangala Shankaregowda currently working as an assistant professor in the Department of Computer Science and Engineering at CHRIST (Deemed to be University) Bangalore. She received her B.E. degree in ISE from Visvesvaraya Technological University, Belgaum and M.Tech. degree in CCT from Mysore University. She is currently pursuing her Ph.D. at Visvesvaraya Technological University (VTU), Belgaum. Her research interests include image processing and deep learning, where she actively explores advancements in these fields. With a strong academic background and a passion for teaching, she contributes significantly to both research and education in computer science. She can be contacted at email: ashagowda05@gmail.com.

Yogish Hullukere Kadegowda is working as professor in the Department of Information Science and Engineering, received B.E. degree in computer science and engineering, from PESCE, Mandya, Mysore University, M.Tech. degree from SJCE Mysore, VTU Belagavi in computer engineering. Ph.D. in computer science from Bharathiar University and PGDCLCF - Post Graduate Diploma in cyber law and cyber forensics - NLSIU (National Law School of Indian University) – Bengaluru. Produced Four Ph.D., and currently guiding 6 scholars for their Ph.D. in VTU. Published and presented 103 papers at National/International Conferences/Journals among 25 papers were Indexed by SCOPUS/Web of Science, 16 IEEE and three papers in DBLP. Two patents and one copy right in his credit. Successfully guided five PhDs and guiding 6 PhD Scholars under VTU. Five Book Chapters Fetches Funds from MODROBS - AICTE (12 Lakhs), DST 7 lakhs. He can be contacted at email: yogishhk@gmail.com